JOURNAL OF CATALYSIS **106**, 125–133 (1987)

# Molybdenum Carbide Catalysts

## I. Synthesis of Unsupported Powders

J. S. LEE,[1] S. T. OYAMA, AND M. BOUDART[2]

*Department of Chemical Engineering, Stanford University, Stanford, California 94305*

Received January 27, 1986; revised February 25, 1987

Temperature-programmed reaction between $MoO_3$ of low specific surface area $S_g$ and a $CH_4/H_2$ mixture produces unsupported powders of hexagonal $Mo_2C$ with $S_g$ from 50 to 100 $m^2\ g^{-1}$ and CO uptake number density of up to $5.0 \times 10^{14}$ $cm^{-2}$. Depending on the preparation conditions, this material can be synthesized with a surface free of contamination by noncarbidic carbon ($Mo_2C$-I) or with a surface completely covered by polymeric carbon layers (C–$Mo_2C$). For the latter case a method of treatment with dihydrogen was developed that removes the carbon contamination to create an active carbide surface ($Mo_2C$-II). © 1987 Academic Press, Inc.

## INTRODUCTION

Many catalytic processes rely on Group VIII metals, in particular on noble metals. As the latter are limited both in quantity and in number of sources, substitutes are of economic and strategic interest. Attractive catalytic substitutes could be based on molybdenum, an inexpensive and widely distributed element. This paper is part of a series of investigations (*1–8*) of supported and unsupported molybdenum and molybdenum carbide catalysts.

With the exception of the second and third rows of Group VIII elements (Ru, Rh, Pd, Ir, and Pt), most transition metals form various carbide and nitride compounds (*9*). Recent reviews show that the combination of a transition metal with carbon or nitrogen atoms yields materials with attractive catalytic activity, stability, selectivity, and resistance to poisoning (*10–12*). However, for the carbide and nitride powders to be used efficiently as catalysts, they must exhibit a high specific surface area $S_g$.

Conventional preparation techniques, inherited from the metallurgical industry, involve the reaction of the metals, metal hydrides, or metal oxides with appropriate amounts of carbon in a protective or reducing atmosphere (*10*). Reaction temperatures are generally very high, e.g., greater than 1500 K for $Mo_2C$. Their low $S_g$ and low purity makes these commercial materials unsuitable as catalysts. Reaction of the metals or their oxides with carburizing gases such as light hydrocarbons or CO has also been used to prepare metallurgical carbides. These materials also exhibit low values of $S_g$ and surfaces contaminated in surface carbon. Another synthetic method, chemical vapor deposition, involves nucleation of gas phase clusters by reacting metal halide or metal carbonyl precursors in various atmospheres including dihydrogen, a hydrocarbon, or an inert gas. Compounds including molybdenum carbide and molybdenum oxycarbide with $S_g$ of 20–60 $m^2\ g^{-1}$ have been made in this way (*2*).

A new synthesis technique to prepare molybdenum carbide and nitride powders has recently been reported (*3–6*). In this process, $MoO_3$ is heated at slowly increasing temperatures in a stream of $CH_4/H_2$ or $NH_3$ to produce $Mo_2C$ and $Mo_2N$ powders with $S_g$ of 51 and 220 $m^2\ g^{-1}$, respectively.

---

[1] Present address: Department of Chemical Engineering, Pohang Institute of Science and Technology, Pohang, Korea.

[2] To whom correspondence should be addressed.

0021-9517/87 $3.00

The latter $S_g$ value represents the highest value on record for an unsupported stable metallic powder (*5*).

Many catalytic reactions have been studied on carbides of Group IV–VI metals, including oxidation, hydrogenation, dehydrogenation, isomerization, hydrogenolysis, and CO–$H_2$ reactions. Results of these early studies have been summarized in recent reviews (*11*, *12*). Many of the previous studies, however, were made on materials with low specific surface areas, typically less than 1 $m^2$ $g^{-1}$. The effects of surface contamination, especially from oxygen and polymeric carbon, have not been well documented. By polymeric carbon is meant surface carbon in amorphous, graphitic, "coke," or other aggregate form. Polymeric carbon is to be differentiated from atomic carbon, which is the form of carbidic carbon in the bulk or on the surface of carbides. Electron paramagnetic resonance and Auger electron spectroscopy show that the surface of tungsten carbide samples consist not only of tungsten and carbidic carbon but also of oxygen and polymeric carbon (*7*). Kojima *et al.* (*13*) found that evacuation above 1270 K activated TaC, TiC, and WC for the hydrogenation of ethylene due to the removal of surface oxygen or oxide as shown by X-ray photoelectron spectroscopy.

Recognition of an analogy between the catalytic behavior of tungsten carbide and that of Group VIII metals has contributed to the interest in the catalytic properties of carbides. In their investigation of isomerization and hydrogenolysis of 1,1,3-trimethylcyclopentane over transition metal films, Muller and Gault (*14*) observed that following an induction period tungsten showed good selectivity toward xylene formation, which was characteristic of the noble metals Pt and Pd, but not of base transition metals. Surface carbide formation during the induction period may explain the unusual behavior of tungsten. Similarity between Pt and WC in their selectivity toward the isomerization of neopentane was also reported (*1*). More recently Leclercq *et al.* (*2*, *8*) found Ru-like behavior of $Mo_2C$ for CO–$H_2$ reactions.

This first paper in a series concerned with supported and unsupported molybdenum and molybdenum carbide catalysts discusses the synthesis of hexagonal $Mo_2C$ unsupported powders with $S_g$ as high as 100 $m^2$ $g^{-1}$. When surface contamination by carbon occurred, the latter was subsequently removed by treatment with dihydrogen under controlled conditions. The CO–$H_2$ reaction and the hydrogenolysis of *n*-butane, to be reported in detail in subsequent papers (*15–16*), were used to test the catalytic properties of these carbide powders.

## EXPERIMENTAL

High purity $MoO_3$ powder (99.998%, Johnson–Matthey) was used as received. Dihydrogen (99.95%, Liquid Carbonic) was purified by diffusion through a heated palladium cell. Helium (99.995%, Liquid Carbonic) and methane (99.97%, Matheson) were purified through 5 Å molecular sieve and MnO/$SiO_2$ traps (*17*), both at room temperature.

The quartz cell was designed to be used both as a synthesis reactor and as an adsorption cell. Its entire volume could be isolated by stopcocks and transferred between a gas delivery system and a volumetric adsorption apparatus without exposure of the sample to air. Each synthesis employed a quantity of 0.1–0.5 g of $MoO_3$ loaded on a coarse quartz fritted disk in the cell and a flow of 50–100 $\mu$mol $s^{-1}$ of a $CH_4$/$H_2$ mixture at atmospheric pressure. A furnace coupled to a controller/programmer heated the cell and a local thermocouple monitored the temperature of the sample. A heating rate of 30 K $h^{-1}$ was generally employed in the syntheses. A higher heating rate of 60 K $h^{-1}$ was also used to obtain greater sensitivity for the measurement of gases produced and consumed during synthesis.

To measure gas adsorption, the cell was isolated and transported to a volumetric adsorption system (*18*) equipped with a Texas Instruments differential pressure gauge. To measure the amount of CO adsorption, the cell was evacuated to $10^{-4}$ Pa at 670 K, and various amounts of CO were dosed sequentially at room temperature (RT) to obtain a first adsorption isotherm. The cell was then evacuated again to $10^{-4}$ Pa at RT for 0.5 h to remove the weakly absorbed CO. Then, a second adsorption isotherm was taken to measure the amount of weakly adsorbed CO. The linear portion of the isotherms was extrapolated to zero pressure and the difference between the two extrapolated values was taken as the amount of strong CO chemisorbed. To determine $H_2$ chemisorption a similar procedure was carried out, but only the first isotherm was taken. Following chemisorption measurements, a physical adsorption isotherm of $N_2$ was measured at liquid nitrogen temperature. Specific surface areas ($S_g$) were calculated by applying the BET equation to the $N_2$ adsorption isotherm in the 5- to 30-kPa pressure range. The BET area was used to estimate the particle size $D_p$ from the equation $D_p = 6/(\rho S_g)$, where $\rho$ is the density of the solid.

The bulk structure of the samples was determined by powder X-ray diffraction (XRD). The crystallite $D_c$ was estimated from application of the Scherrer equation $D_c = \lambda/(\beta \cos \theta)$, where $\lambda$ represents the wavelength of the X-ray radiation, $\theta$ the Bragg angle, and $\beta$ the width of the XRD peak at half-maximum corrected for $K_\alpha$-doublet separation and instrumental broadening. The 2–3 major peaks used in the calculation yielded similar values of $D_c$. Samples were passivated with flowing 1% $O_2$ in He at RT before removal from the cell for XRD.

The gas products obtained during the temperature-programmed reaction (TPR) experiments were analyzed with a gas chromatograph (Hewlett–Packard 5980) equipped with thermal conductivity and flame ionization detectors. A 2.5-m-long, 3-mm-diameter Chromosorb 102 column was used. A peak integrator (Hewlett–Packard 3600) was used to determine chromatograph peak areas.

## RESULTS

### *Preparation of Hexagonal $Mo_2C$ by TPR of $MoO_3$*

The preparation of $Mo_2C$ was accomplished by TPR of $MoO_3$ in a flowing $CH_4/H_2$ mixture. The rate of heating, the final temperature of the TPR, the flow rate of gases, and the $CH_4/H_2$ ratio are variables that determine the properties of the $Mo_2C$ product.

Figure 1a shows a typical TPR profile of the synthesis process utilizing a 20% $CH_4/H_2$ mixture supplied at the rate of 68 μmol $s^{-1}$ over 0.5 g (5200 μmol) of $MoO_3$. It was found that no changes occurred in the materials below 550 K, so the samples were quickly brought to this temperature and were then further heated at a rate of 60 K $h^{-1}$. As a comparison, Fig. 1b shows the TPR profile for the reduction process utilizing pure $H_2$ at identical conditions of flow

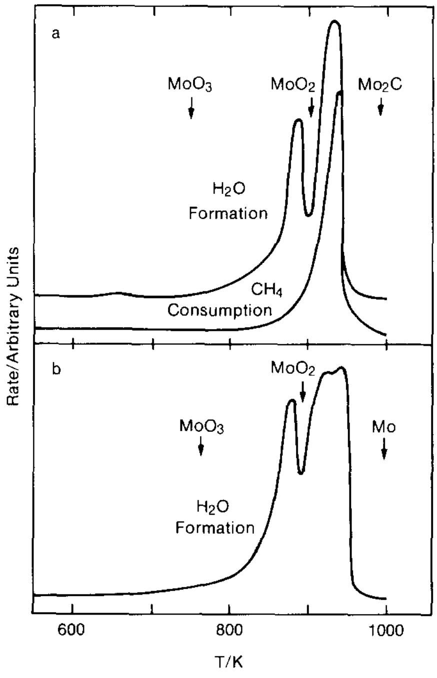

FIG. 1. TPR traces of coreduction/carburization of $MoO_3$ (a) in flowing 20% $CH_4/H_2$ mixture, (b) in flowing $H_2$ only. The TPR conditions in both cases are $MoO_3$ loading, 0.5 g; total flow rate, 68 μmol $g^{-1}$; heating rate, 60 K $h^{-1}$.

rate, reactant loading, and heating rate as employed in the synthesis process.

The rates of water formation and methane consumption were obtained by monitoring the gas composition at the reactor outlet with a gas chromatograph. For both synthesis and reduction processes the rate of water formation showed two peaks, the first of which occurred at the same temperature. When TPR was halted after this first peak, the material in both processes was found by XRD to be essentially all $MoO_2$. When TPR was halted prior to the first peak, several suboxides of $MoO_3$ were detected. Thus, both the synthesis and the reduction processes go through a common first stage of formation of $MoO_2$.

In the case of the synthesis of $Mo_2C$, the carbon is incorporated into the solid during a second stage, indicated by a coincident second water formation peak and a methane consumption peak. In the case of reduction to Mo, the reaction also proceeds through a second stage in which $H_2$ is consumed to produce a second water formation peak. Indeed, when a TPR of $MoO_2$ (99.0%, Alfa) was carried out, this second peak alone was produced. The carburization by TPR with a 20% $CH_4/H_2$ mixture produced hexagonal $Mo_2C$ with $S_g$ of 60 $m^2$ $g^{-1}$, while the TPR with $H_2$ produced Mo metal with $S_g$ of 3 $m^2$ $g^{-1}$ as measured by XRD and the $N_2$ BET method.

Thermodynamics was used as a guide to prepare the carbide without surface contamination due to polymeric carbon. Figure 2 shows the plot of equilibrium relationships at atmospheric pressure for the reactions

(a) $C(graphite) + 2H_2 = CH_4$
(b) $Mo_2C + 2H_2 = 2Mo + CH_4$

By maintaining preparation conditions within the region between curves (a) and (b), it should be possible to prepare $Mo_2C$ without forming graphitic carbon. The operating line employed to prepare an initially clean $Mo_2C$ sample ($Mo_2C$-I) in one step is indicated in Fig. 2. The endpoint was determined by first running a preliminary synthesis with an arbitrary positive $CH_4/H_2$ ratio to determine the temperature required for carbide formation, and then choosing at this temperature the highest $CH_4/H_2$ ratio that would not cross curve (a). This provides the maximum driving force for carbon supply while avoiding the formation of polymeric carbon. With a heating rate of 30 K $h^{-1}$ the required endpoint was found to be 930 K with a methane concentration of 20%. The product, $Mo_2C$-I, had an $S_g$ of 60 $m^2$ $g^{-1}$ and a CO uptake at RT of 220 $\mu$mol $g^{-1}$. When the preparation was made isothermally at 930 K, keeping other conditions identical to the TPR preparation, the $Mo_2C$ was produced with an $S_g$ of 5 $m^2$ $g^{-1}$.

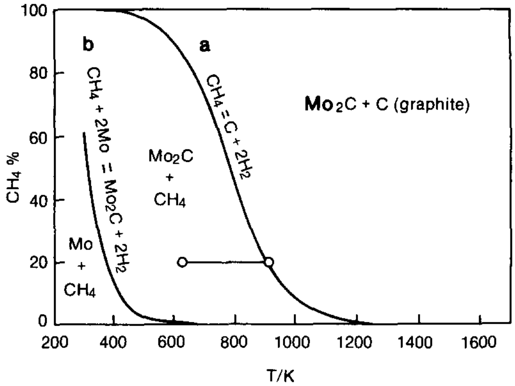

FIG. 2. Equilibrium relationships at atmospheric pressure for the reactions (a) $C(graphite) + 2H_2 = CH_4$ and (b) $Mo_2C + 2H_2 = 2Mo + CH_4$. Thermodynamic data were obtained from I. Barin and O. Knacke, "Thermochemical Properties of Inorganic Substances," Springer-Verlag, Berlin, 1973.

### *Cleaning of $Mo_2C$ Surfaces Contaminated by Polymeric Carbon*

Figure 3 shows TPR profiles of the reaction between $H_2$ and $Mo_2C$ powders with varying amounts of surface carbon. The $Mo_2C$-I sample showed one methane peak at 735 K. The area under this peak corresponded to an atomic ratio of $C/Mo_s$ of 0.6, with $Mo_s$ denoting a surface Mo atom. It was assumed that 1 $m^2$ of surface area determined by the BET method contained $10^{19}$

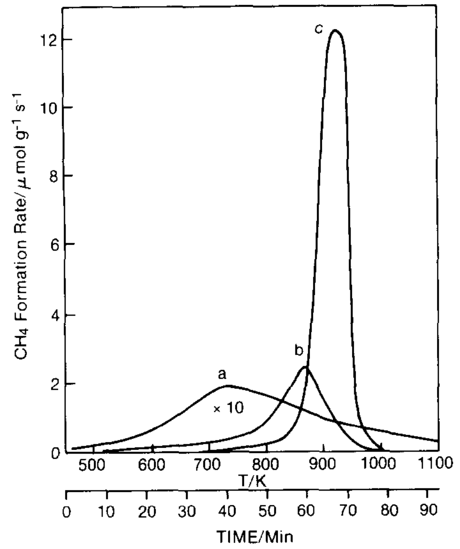

FIG. 3. TPR traces for the removal of surface carbon from $Mo_2C$ powders by reaction with $H_2$. Heating rate was 430 K $h^{-1}$. (a) $Mo_2C$-I ($C/Mo_s = 0.6$), (b) $Mo_2C$-II ($C/Mo_s = 2.4$), (c) C–$Mo_2C$ ($C/Mo_s = 6.4$). The amount of surface carbon ($C/Mo_s$) removed by TPR was established from peak areas.

surface Mo atoms. Since this amount is close to the ideal stoichiometry of $Mo_2C$ ($C/Mo = 0.5$), and bulk carbon is unreactive in this temperature range (*19*), it is believed that only surface carbon consisting of carbidic carbon was removed. However, for the preparation of the sample labeled C–$Mo_2C$, either higher final temperatures or higher methane concentrations in the feed mixture were used than were employed for $Mo_2C$-I, and polymeric carbon was deposited. The TPR of C–$Mo_2C$ showed a methane peak at a much higher temperature, 920 K, and the amount of carbon removed corresponded to a $C/Mo_s$ ratio of 6.4, indicating that multilayer deposits of polymeric carbon were present.

The BET areas and CO uptakes were measured for intermediate stages of TPR of C–$Mo_2C$, and the results are shown in Fig. 4. Initially, no CO was chemisorbed. As carbon was removed at increasing temperatures in the form of methane, CO chemisorption increased and peaked at approximately the same temperature as the peak temperature of methane formation in TPR. A similar trend was observed for the change in $S_g$, except that its value at this peak temperature was only 20–30% higher than that of the initial sample. After TPR up to 1200 K, XRD showed that part of the $Mo_2C$ was converted to Mo.

Results of an isothermal $H_2$ treatment of C–$Mo_2C$ at 875 K are shown in Fig. 5b. In this case the effect on $S_g$ and CO uptake of increasing the time of exposure of the sample to $H_2$ was similar to that of increasing the temperature in the TPR experiment. However, relatively high $S_g$ and CO uptakes were still maintained until the end of the treatment. The behavior of $Mo_2C$-I in the isothermal $H_2$ treatment (Fig. 5a) was completely different. A continuous decrease in $S_g$ and CO chemisorption was observed. After 5 h of $H_2$ treatment at 875 K, both C–$Mo_2C$ and $Mo_2C$-I showed XRD patterns corresponding only to $Mo_2C$. The isothermal $H_2$ treatment thus provides not only a method to clean surfaces contaminated by polymeric carbon, but also a new procedure to prepare $Mo_2C$ ($Mo_2C$-II) from C–$Mo_2C$. By interrupting the $H_2$ treatment immediately after observing the maximum of methane formation, one can obtain pure $Mo_2C$ samples with the highest values of $S_g$ and CO uptake.

Figure 6 shows the effect on the product

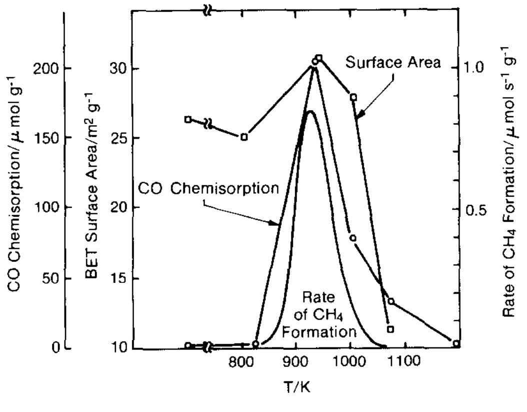

FIG. 4. The change in BET surface area (□), and the amount of CO chemisorption (○), during TPR of C–$Mo_2C$ with flowing $H_2$. Heating rate was 60 K $h^{-1}$.

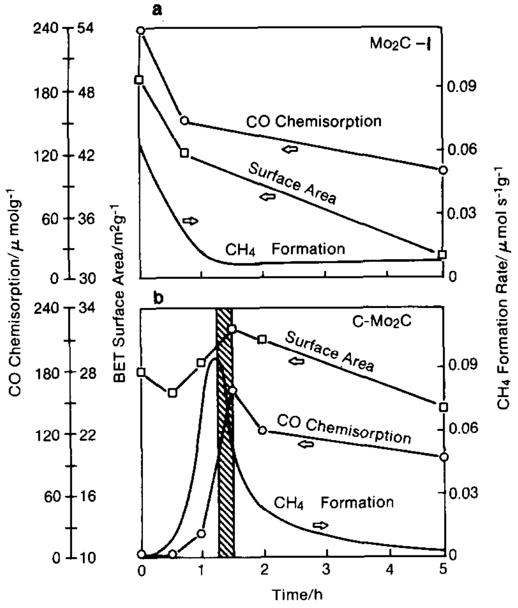

FIG. 5. The change in BET surface area (□), and the amount of CO chemisorption (○), during isothermal $H_2$ treatment at 875 K. (a) $Mo_2C$-I; (b) C–$Mo_2C$. The treatment of C–$Mo_2C$ could be interrupted immediately after observing the maximum rate of methane formation (around the shaded area in b) to prepare $Mo_2C$-II.

$S_g$ of methane concentration in the feed gas mixture during carburization by TPR of $MoO_3$. The $S_g$ of the samples prepared with methane concentration higher than 20% was measured after the cleaning treatment with $H_2$ at 875 K. A Mo metal sample prepared in pure $H_2$ is also shown for comparison. A good correlation is seen between methane concentration and $S_g$: a higher methane concentration yields $Mo_2C$ with a higher $S_g$. A higher final temperature (>1020 K) was needed for complete reduction when 100% methane was used, possibly because dissociation of methane is more difficult than dissociation of $H_2$. However, this process using 100% methane produced $Mo_2C$ with the highest value of $S_g$, i.e., 100 $m^2\ g^{-1}$.

### *Adsorption Properties of $Mo_2C$ Powders*

TABLE 1

Characterization of Typical $Mo_2C$ Powders

| | $Mo_2C$-I | $Mo_2C$-II |
|---|---|---|
| $S_g$ ($m^2\ g^{-1}$) | 60 | 84 |
| Chemisorption (μmol $g^{-1}$) | | |
| CO | 218 | 505 |
| $H_2$ | 100 | — |
| Number density ($10^{14}\ cm^{-2}$) | | |
| $n_{CO}$ | 2.2 | 3.6 |
| $n_{H_2}$ | 1.0 | — |
| Particle size (nm) | | |
| $D_p$ by BET | 11.0 | 8.0 |
| $D_c$ by X ray | 11.5 | 5.8 |

Table 1 shows the properties of two types of $Mo_2C$ powders. The $Mo_2C$-I sample was prepared in one step using 20% $CH_4/H_2$ in a TPR/carburization. The $Mo_2C$-II sample was prepared with 80% $CH_4/H_2$, and was activated by isothermal $H_2$ treatment at 875 K. The latter has a higher $S_g$ value. The number density of CO ($n_{CO}$) and $H_2$ ($n_{H_2}$) was calculated as the amount of gas uptake per unit surface area. The $Mo_2C$-II sample had a higher number density as well. When $Mo_2C$-I was treated in $H_2$ at 550–650 K,

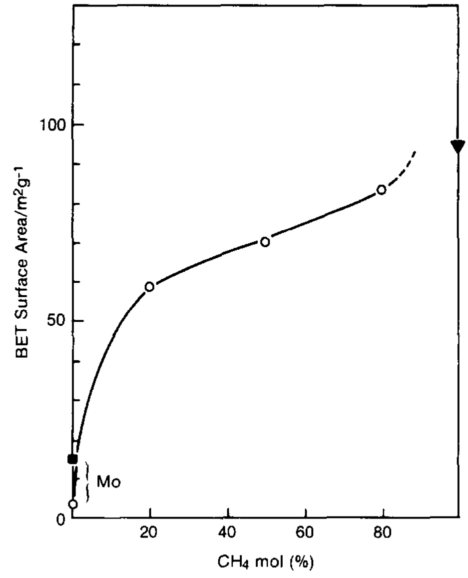

FIG. 6. BET surface areas of $Mo_2C$ powders produced by TPR/carburization with different $CH_4/H_2$ mixtures. In all TPR, heating rate was 30 K $h^{-1}$. (○, TPR between 670 and 950 K; ▼, TPR between 670 and 1020 K; ■, isothermal reduction in flowing $H_2$ at 770 K for 30 h.

however, its value of $n_{CO}$ increased to $5.0 \times 10^{14}$ $cm^{-2}$. The adsorption stoichiometry for CO is lower than that expected for molecular adsorption on the molybdenum surface, but is consistent with that for dissociative adsorption. However, dissociative adsorption of CO was not found in the case of CO adsorption on carburized Mo(100) (*20*). Thus, the presence of some surface carbon that suppresses chemisorption is possible.

The value of $n_{H_2}$ for $Mo_2C$-I is lower than that of $n_{CO}$. Furthermore, unlike CO chemisorption, $H_2$ adsorption was not equilibrated after 10 h of exposure of the sample to 20 kPa of $H_2$. The reported $n_{H_2}$ value was based on the $H_2$ uptake during this period. The slowness of $H_2$ compared to CO chemisorption is qualitatively consistent with the findings of Ko and Madix (*20*), who observed that $H_2$, but not CO chemisorption, is suppressed under ultrahigh-vacuum conditions by carburizing the Mo(100) surface.

## DISCUSSION

### *Synthesis of High Surface Area Carbides without Surface Contamination*

A TPR with a $CH_4/H_2$ mixture provides a new procedure for synthesizing a high surface area molybdenum carbide, $Mo_2C$, from a low surface area oxide, $MoO_3$. The mechanism of this coreduction/carburization is not clear. A first stage is the formation of an intermediate $MoO_2$ phase. Later stages may involve the breakage of large oxide particles due to the growth of separate carbidic and metallic phases within the same particle. There is no apparent topotactic phenomenon as in the case of the synthesis of $Mo_2N$ from $MoO_3$ (*5*). Two criteria should be satisfied to obtain a high $S_g$ material. First, each step in the solid transformation should proceed at the lowest possible temperature so as to minimize the unnecessary movement of species which leads to growth of particles. This occurs in topotactic transformations (*5, 6*). A slow TPR is suitable for this purpose, but the rate of heating should not be too slow because long preparation times may also allow particle growth. Second, metallic intermediates should be avoided. Metals have lower Tammann temperatures than their carbides and thus greater tendency to sinter. The whole process of coreduction/carburization can be viewed as a kinetic competition between rates of oxygen transport out and carbon transport in and rates of particle growth. With a sufficiently high methane concentration, the rate of diffusion of carbon atoms is high enough so that the carbide phase is formed without passage through a metallic phase and, thus, before loss of surface area. Indeed, in the preparation of $Mo_2C$ from $MoO_3$, when $CH_4$ concentration is low, both Mo metal and $Mo_2C$ are formed and a material low in $S_g$ results. With increasing $CH_4$ concentration a monotonic increase in $S_g$ is observed (Fig. 6). Presumably, at high $CH_4$ concentrations, oxygen from the molybdenum oxide precursor is removed as CO and $CO_2$ as well as $H_2O$. This removal does not appear to be limiting, as the highest surface areas are obtained at high $CH_4$ concentrations.

Thermodynamics can be used as a guide to prepare transition metal carbides without surface contamination by polymeric carbon. There are, however, limitations to the application of this thermodynamic guideline. First, if there exist reactions that deposit polymeric carbon in an irreversible manner, equilibrium arguments are invalidated. Second, for a given oxide to carbide transformation, the $CH_4$–graphite equilibrium curve gives the $CH_4$ concentration that should be used to avoid polymeric carbon deposition. However, if the temperature of the oxide to carbide transformation is too high, the required methane concentration may be too low and the reaction may be starved in carbon reactant. But because of the stoichiometry of both reactions considered in Fig. 2, the equilibrium curves are shifted to higher temperatures as the pressure is increased. Thus, in principle, it is possible to overcome the mass transport problem by increasing the pressure of the preparation. Alternatively, a method can be used for removing the carbon from the surface. This approach is discussed in the following section.

### *Cleaning of Carbide Surfaces Contaminated by Polymeric Carbon: A Method for the Preparation of Carbides with High $S_g$*

The isothermal $H_2$ activation whereby the $H_2$ treatment is interrupted immediately after observing maximum methane formation was shown to clean carbon-contaminated $Mo_2C$. During the $H_2$ treatment preceding this maximum rate of methane formation, CO chemisorption sites are formed by removing polymeric carbon layers, and $S_g$ also increases since pore mouths blocked by carbon are cleared. Once the process passes throughout the peak of methane formation, further $H_2$ treatment only results in a decrease in $S_g$ and CO chemisorption (Fig. 4). The drop in CO chemisorption after the peak of methane formation between 930 and 1000 K is substantially larger than the decrease in surface area. This may be due to surface contamination as a result of the previous chemisorption measurements on the same sample. For $Mo_2C$-I which initially has a clean surface, the $H_2$ treatment only decreases $S_g$ and CO chemisorption. Figure 7 shows a schematic representation of the process. The $Mo_2C$-II prepared by this process still contains polymeric carbon on its surface since only about half of the initial carbon on C–$Mo_2C$ was removed and C/$Mo_s$ is 2.4 (Fig. 3b). However, a clean surface is now exposed, permitting a large CO chemisorption on this sample.

It is interesting to note that $Mo_2C$ catalyzes the removal of polymeric carbon by dihydrogen. The change in methane formation rate shown in Fig. 5b represents a typical autocatalytic behavior. Catalytic sites are generated by the reaction itself and rate increases until the depletion of reactant carbon retards the rate again. It is shown elsewhere (*21*) that $Mo_2C$ is actually as good as Pt as a catalyst for the hydrogenolysis of bulk carbon.

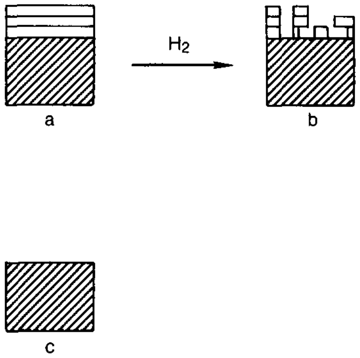

FIG. 7. Schematic representation of (a) C–$Mo_2C$, (b) $Mo_2C$-II, and (c) $Mo_2C$-I. Shaded blocks represent ideal $Mo_2C$, on the top of which polymeric carbon layers are formed.

Since a method is available to clean $Mo_2C$ covered by polymeric carbon, high concentrations of methane in $H_2$ can now be used in the preparation of $Mo_2C$ powders. A good correlation in Fig. 6 between percent methane in the feed mixture and $S_g$ of the produced carbide supports the validity of the guidelines proposed in the previous section: by increasing the driving force for carbon supply, the chance for the formation of a metallic intermediate is reduced, giving higher $S_g$ products.

## ACKNOWLEDGMENTS

This work was initiated with support from NSF through the Center for Materials Research at Stanford University under the NSF-MRL Program. It has been completed with the help of DOE grant DE-AT03-79ER10502-03.

## REFERENCES

*1.* Boudart, M., and Levy, R., *Science* **181,** 547 (1973).
*2.* Leclercq, L., Imura, K., Yoshida, S., Barbee, T., and Boudart, M., *in* "Preparation of Catalysts II" (B. Delmon, P. Grange, P. A. Jacobs, and G. Poncelet, Eds.), p. 627. Elsevier, Amsterdam, 1978.
*3.* Oyama, S. T., Ph.D. dissertation, Stanford University, 1981.
*4.* Volpe, L., Oyama, S. T., and Boudart, M., *in*

"Preparation of Catalysts III" (G. Poncelet and P. A. Jacobs, Eds.), p. 147. Elsevier, Amsterdam, 1983.

5. Volpe, L., and Boudart, M., *J. Solid State Chem.* **59,** 332 (1985).
6. Volpe, L., and Boudart, M., *J. Solid State Chem.* **59,** 348 (1985).
7. Boudart, M., Lee, J. S., Imura, K., and Yoshida, S., *J. Catal.* **103,** 30 (1987).
8. Boudart, M., Oyama, S. T., and Leclercq, L., *in* "Proceedings, 7th International Congress on Catalysis, Tokyo, 1980" (T. Seiyama and K. Tanabe, Eds.), p. 578. Elsevier, Amsterdam, 1981.
9. Toth, L. E., "Transition Metal Carbides and Nitrides." Academic Press, New York, 1971.
10. Levy, R. B., *in* "Advanced Materials in Catalysis" (J. J. Burton and R. L. Garten, Eds.), p. 101. Academic Press New York, 1977.
11. Oyama, S. T., and Haller, G. L., *Catalysis* (Spec. Per. Repts., Roy. Soc. Chem., London) **5,** 333 (1982).
12. Leclercq, L., *in* "Surface Properties and Catalysis by Non-metals" (J. P. Bonnelle, B. Delmon, and E. Derouane, Eds.), p. 433. Reidel, Dordrecht, 1983.
13. Kojima, I., Miyazaki, E., Inoue, Y., and Yasumori, I., *J. Catal.* **59,** 472 (1979).
14. Muller, J. M., and Gault, F. G., *Bull. Soc. Chim. Fr.* **2,** 416 (1970).
15. Lee, J. S., Locatelli, S., Boudart, M., and Oyama, S. T., in preparation.
16. Lee, J. S., Locatelli, S., and Boudart, M., *J. Catal.*, in preparation.
17. McIlwrick, C. R., and Phillips, C. S. G., *J. Phys.* **E6,** 1208 (1973).
18. Hanson, F. V., Ph.D. dissertation, Stanford University, 1975.
19. Holstein, W. L., and Boudart, M., *J. Catal.* **72,** 328 (1981).
20. Ko, E. I., and Madix, R. J., *Surf. Sci.* **109,** 221 (1981).
21. Lee, J. S., and Boudart, M., *J. Catal.*, submitted.